

LMC X-4 is a massive binary system comprising an 07III-V or 08III-V star<sup>21,26</sup> with a mass of  $\sim 17 M_{\odot}$  together with a  $\sim 1.6 M_{\odot}$  neutron star<sup>27</sup> in orbit with a 1.408-day period. The X-ray source has occasional flaring episodes during which  $\sim 30\%$  of the X rays are pulsed<sup>27</sup> with a period of 13.5 s, presumably the spin period of the neutron star. The inclination<sup>27</sup> of the system is  $\sim 66^{\circ}$  and the X-ray source is eclipsed between phase 0.92 and 0.08. If UHE protons are accelerated in the region of the compact object UHE  $\gamma$  rays could be produced by nuclear interactions in the atmosphere of the companion star. In this case, we would expect  $\gamma$ -ray emission at orbital phases  $\sim 0.92$  and  $0.08$  when our line-of-sight to the neutron star just grazes the star's surface. The observation of UHE  $\gamma$  rays at a phase of 0.90-0.95 is consistent with this picture, although the absence of UHE emission at phases 0.05-0.10 is puzzling (a similar situation exists for Cyg X-3 and Vela X-1 where only one burst of UHE  $\gamma$  rays is observed per orbit). The X-ray source has high and low states associated with a 30.5-day period<sup>22</sup> attributed to precession of an accretion disk. This precessing disk picture is supported by ultraviolet observations<sup>28</sup> which indicate an almost constant X-ray heating of the stellar atmosphere.

The star does not appear to fill its Roche lobe<sup>21</sup> and seems to have a rather low stellar wind<sup>21,28</sup>. Mass transfer may occur through a trailing accretion stream<sup>21</sup> which may feed the accretion disk. Evidence for this comes from variable obscuration of the companion star<sup>21</sup> between orbital phases 0.6 and 0.9 corresponding to matter trailing behind the neutron star by between 0.2 and 0.3 of an orbit. If this matter is of considerable extent above the orbital plane it could be the target material for interactions of UHE protons produced near the neutron star. Such a scenario would produce  $\gamma$  rays only at a phase of  $\sim 0.9$  as observed.

We conclude that we have found evidence for UHE  $\gamma$ -ray emission by the LMC X-4 system modulated with the 1.408-day orbital period. The emission occurs when the neutron star is just entering its eclipse by the companion star and could result from nuclear interactions in the atmosphere of the companion by UHE particles produced near the neutron star. Alternatively, a trailing accretion stream could provide target material and explain the absence of UHE  $\gamma$  rays on leaving eclipse. Further observations in progress above  $10^{15}$  and  $10^{16}$  eV coupled with observations from a more southerly site at about  $10^{14}$  eV could provide a test for the universality of the microwave background, be used as an indirect measurement of the magnetic field between our Galaxy and the Large Magellanic Cloud, or provide an independent measurement of the distance to the Large Magellanic Cloud.

We acknowledge the efforts of P. R. Gerhardy in obtaining the data-base analysed in the present work. Others particularly responsible for the development of the Buckland Park array have been J. R. Prescott, J. R. Patterson, A. G. Gregory, P. C. Crouch and D. F. Liebing. We thank D. F. Liebing and A. A. Watson for helpful comments and K. J. Orford and K. E. Turver for helpful discussions. R.J.P. thanks the Australian Government for a Queen Elizabeth II Fellowship. This work was supported in part by the Australian Research Grants Committee.

Received 22 November 1984; accepted 6 March 1985.

- Samorski, M. & Stamm, W. *Astrophys. J. Lett.* **268**, L17-L22 (1983).
- Lloyd-Evans, J. *et al. Nature* **305**, 784-787 (1983).
- Protheroe, R. J., Clay, R. W. & Gerhardy, P. R. *Astrophys. J. Lett.* **280**, L47-L50 (1984).
- Eichler, D. & Vestrand, W. T. *Nature* **307**, 613-614 (1984).
- Stephens, S. A. & Verma, R. P. *Nature* **308**, 828-830 (1984).
- Protheroe, R. J. *Nature* **310**, 296-298 (1984).
- Hillas, A. M. *Nature* **312**, 50-51 (1984).
- Wdowczyk, J. & Wolfendale, A. W. *Nature* **305**, 609-610 (1983).
- Wdowczyk, J. & Wolfendale, A. W. *Nature* **306**, 347-349 (1983).
- Crouch, P. C. *et al. Nucl. Instrum. Meth.* **179**, 467-476 (1981).
- Gerhardy, P. R. & Clay, R. W. *J. Phys. G: Nucl. Phys.* **9**, 1279-1287 (1983).
- Clay, R. W. & Gerhardy, P. R. *Aust. J. Phys.* **35**, 59-65 (1982).
- Clay, R. W., Protheroe, R. J. & Gerhardy, P. R. *Nature* **309**, 687-688 (1984).
- Protheroe, R. J. & Clay, R. W. *Proc. Astr. Soc. Aust.* **5**, 586-589 (1984).
- Gawin, J., Maze, R., Wdowczyk, J. & Zawadzki, A. *Can. J. Phys.* **46**, S75-S77 (1968).
- Protheroe, R. J. *Astr. Expt.* (submitted).
- Protheroe, R. J. *Astr. Expt.* **1**, 33-38 (1984).
- Wdowczyk, J. *et al. Proc. 12th Int. Cosmic Ray Conf. (Hobart)* **3**, 965-967 (1971).

- Gould, R. J. *Astrophys. J. Lett.* **274**, L23-L25 (1983).
- van der Klis, M. *et al. Astr. Astrophys.* **106**, 339-344 (1982).
- Huchings, J. B., Crampton, D. & Cowley, A. P. *Astrophys. J. Lett.* **225**, 548-556 (1978).
- Lang, F. L. *et al. Astrophys. J. Lett.* **246**, L21-L25 (1981).
- Bradt, H. V. & McClintock, J. E. *A. Rev. Astr. Astrophys.* **21**, 13-66 (1983).
- Prescott, J. R. *et al. Proc. 18th Int. Cosmic Ray Conf. Bangalore* **6**, 257-260 (1983).
- Cawley, M. F., Gibbs, K. & Weekes, T. C. *Proc. 18th Int. Cosmic Ray Conf. Bangalore* **9**, 69-72 (1983).
- Chevalier, C. & Ilovaisky, S. A. *Astr. Astrophys.* **59**, L9-L12 (1977).
- Kelley, R. L. *et al. Astrophys. J.* **264**, 568-574 (1983).
- van der Klis, M. *et al. Astr. Astrophys.* **106**, 339-344 (1982).
- Skinner, G. K. *Space Sci. Rev.* **30**, 441-446 (1981).
- van der Klis, M., Tjemkes, S. & van Paradijs, J. *Astr. Astrophys.* **126**, 265-268 (1983).
- Huchings, J. B., Crampton, D. & Cowley, A. P. *Astrophys. J. Lett.* **275**, L43-L47 (1983).
- Cowley, A. P., Crampton, D. & Huchings, J. B. *Astrophys. J.* **256**, 605-611 (1982).
- Murakami, T. *et al. Astrophys. J.* **264**, 563-567 (1983).
- Priedhorsky, W. C. & Terrell, J. *Astrophys. J.* **273**, 709-715 (1983).
- Thomas, R. M. *et al. Mon. Not. R. Astr. Soc.* **185**, 29P-32P (1978).
- Davison, P. J. N. *et al. Mon. Not. R. Astr. Soc.* **181**, 73P-79P (1977).
- Gottlieb, E. W., Wright, E. L. & Liller, W. *Astrophys. J. Lett.* **195**, L33-L35 (1975).
- Middleditch, J. *et al. Astrophys. J.* **244**, 1001-1021 (1981).
- van Paradijs, J. *et al. Astr. Astrophys. Suppl.* **55**, 7-14 (1984).

## Large losses of total ozone in Antarctica reveal seasonal ClO<sub>x</sub>/NO<sub>x</sub> interaction

J. C. Farman, B. G. Gardiner & J. D. Shanklin

British Antarctic Survey, Natural Environment Research Council, High Cross, Madingley Road, Cambridge CB3 0ET, UK

Recent attempts<sup>1,2</sup> to consolidate assessments of the effect of human activities on stratospheric ozone (O<sub>3</sub>) using one-dimensional models for 30° N have suggested that perturbations of total O<sub>3</sub> will remain small for at least the next decade. Results from such models are often accepted by default as global estimates<sup>3</sup>. The inadequacy of this approach is here made evident by observations that the spring values of total O<sub>3</sub> in Antarctica have now fallen considerably. The circulation in the lower stratosphere is apparently unchanged, and possible chemical causes must be considered. We suggest that the very low temperatures which prevail from midwinter until several weeks after the spring equinox make the Antarctic stratosphere uniquely sensitive to growth of inorganic chlorine, ClX, primarily by the effect of this growth on the NO<sub>2</sub>/NO ratio. This, with the height distribution of UV irradiation peculiar to the polar stratosphere, could account for the O<sub>3</sub> losses observed.

Total O<sub>3</sub> has been measured at the British Antarctic Survey stations, Argentine Islands 65°S 64°W and Halley Bay 76°S 27°W, since 1957. Figure 1a shows data from Halley Bay. The mean and extreme daily values from October 1957 to March 1973 and the supporting calibrations have been discussed elsewhere<sup>4,5</sup>. The mean daily value for the four latest complete observing seasons (October 1980-March 1984) and the individual daily values for the current observing season are detailed in Fig. 1. The more recent data are provisional values. Very generous bounds for possible corrections would be  $\pm 30$  matm cm. There was a changeover of spectrophotometers at the station in January 1982; the replacement instrument had been calibrated against the UK Meteorological Office standard in June 1981. Thus, two spectrophotometers have shown October values of total O<sub>3</sub> to be much lower than March values, a feature entirely lacking in the 1957-73 data set. To interpret this difference as a seasonal instrumental effect would be inconsistent with the results of routine checks using standard lamps. Instrument temperatures (recorded for each observation) show that the March and October operating conditions were practically identical. Whatever the absolute error of the recent values may be, within the bounds quoted, the annual variation of total O<sub>3</sub> at Halley Bay has undergone a dramatic change.

Figure 1b shows data from Argentine Islands in a similar form, except that for clarity the extreme values for 1957-73 have been omitted. The values for 1980 to the present are provisional, the extreme error bounds again being  $\pm 30$  matm cm. The

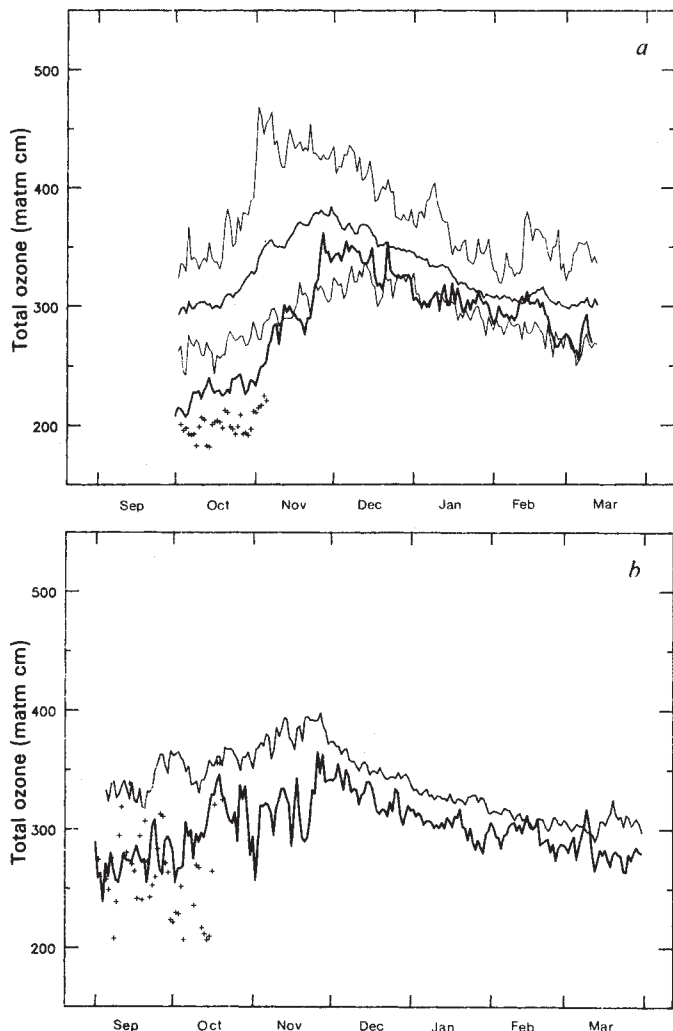


**Fig. 1** Daily values of total  $O_3$ . *a*, Halley Bay: thin lines, mean and extreme values for 16 seasons, 1957-73; thick line, mean values for four seasons, 1980-84; +, values for October 1984. Observing season: 1 October to 13 March. *b*, Argentine Islands: as for Halley Bay, but extreme values for 1957-73 omitted. Observing season: 1 September to 31 March.

changes are similar to those seen at Halley Bay, but are much smaller in magnitude.

Upper-air temperatures and winds are available for these stations from 1956. There are no indications of recent departures from established mean values sufficient to attribute the changes in total  $O_3$  to changes in the circulation. The present-day atmosphere differs most prominently from that of previous decades in the higher concentrations of halocarbons. Figure 2*a* shows the monthly mean total  $O_3$  in October at Halley Bay, for 1957-84, and Fig. 2*b* that in February, 1958-84. Tropospheric concentrations of the halocarbons F-11 ( $CFCl_3$ ) and F-12 ( $CF_2Cl_2$ ) in the Southern Hemisphere<sup>3</sup> are also shown, plotted to give greatest emphasis to a possible relationship. Their growth, from which increase of stratospheric CIX is inferred, is not evidently dependent on season. The contrast between spring and autumn  $O_3$  losses and the striking enhancement of spring loss at Halley Bay need to be explained. In Antarctica, the lower stratosphere is ~40 K colder in October than in February. The stratosphere over Halley Bay experiences a polar night and a polar day (many weeks of darkness, and of continuous photolysis, respectively); that over Argentine Islands does not. Figure 3 shows calculated amounts of  $NO_x$  in the polar night and the partitioning between the species<sup>6</sup> Of these, only  $NO_3$  and  $NO_2$  are dissociated rapidly by visible light. The major reservoir,  $N_2O_5$ , which only absorbs strongly below 280 nm, should be relatively long-lived. Daytime

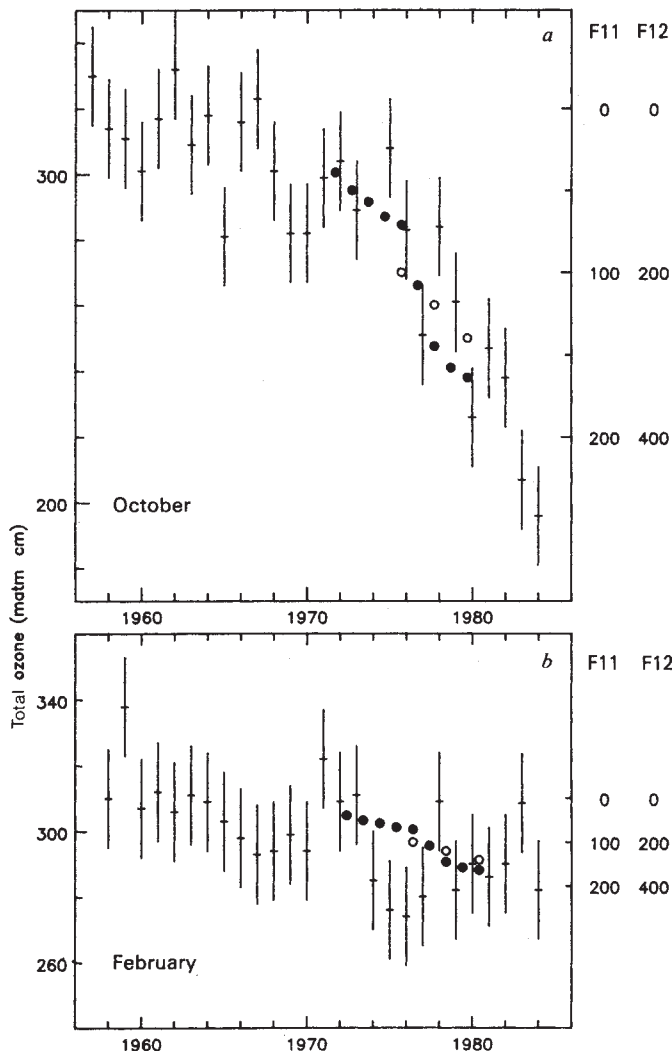


**Fig. 2** Monthly means of total  $O_3$  at Halley Bay, and Southern Hemisphere measurements of F-11 ( $\bullet$ , p.p.t.v. (parts per thousand by volume)  $CFCl_3$ ) and F-12 ( $\circ$ , p.p.t.v.  $CF_2Cl_2$ ). *a*, October, 1957-84. *b*, February, 1958-84. Note that F-11 and F-12 amounts increase down the figure.

levels of  $NO$  and  $NO_2$  should be much less in early spring, following the polar night, than in autumn, following the polar day. Recent measurements<sup>7</sup> support these inferences. The effect of these seasonal variations on the strongly interdependent  $ClO_x$  and  $NO_x$  cycles is examined below.

The  $O_3$  loss rate resulting from  $NO_x$  and  $ClO_x$  may be written<sup>8</sup>

$$L = N + C = 2k_2[O][NO_2] + 2k_6[O][ClO] \quad (1)$$

$L$  accounts for over 85% of  $O_3$  destruction in the altitude range 20-40 km. At 40 km,  $N$  and  $C$  are roughly equal. Lower down,  $C$  decreases rapidly to 10% of  $L$  at 30 km, 3% at 20 km (refs 6, 8). Equation (1) is based on two steady-state approximations, (see Table 1*a* for the reactions involved)

$$\psi = \frac{[NO_2]}{[NO]} \sim \frac{k_1[O_3] + k_4[ClO]}{k_2[O] + j_3} \quad (2)$$

and

$$\chi = \frac{[Cl]}{[ClO]} \sim \frac{k_6[O] + k_4[NO]}{k_5[O_3]} \quad (3)$$

valid in daytime, with  $[O]$  in steady state with  $[O_3]$ . Reaction (4) has a negative temperature coefficient, whereas reaction (1)

**Table 1** Reaction list

<b>a</b> Governing $\psi$ and $\chi$ (see text)	
$\text{NO} + \text{O}_3 \rightarrow \text{NO}_2 + \text{O}_2$	(1)
$\text{NO}_2 + \text{O} \rightarrow \text{NO} + \text{O}_2$	(2)
$\text{NO}_2 + h\nu \rightarrow \text{NO} + \text{O}$	(3)
$\text{NO} + \text{ClO} \rightarrow \text{NO}_2 + \text{Cl}$	(4)
$\text{Cl} + \text{O}_3 \rightarrow \text{ClO} + \text{O}_2$	(5)
$\text{ClO} + \text{O} \rightarrow \text{Cl} + \text{O}_2$	(6)
<b>b</b> Governing $[\text{Cl} + \text{ClO}]$	
$\text{HCl} + \text{OH} \rightarrow \text{Cl} + \text{H}_2\text{O}$	(7)
$\text{ClONO}_2 + h\nu \rightarrow \text{Cl} + \text{NO}_2$	(8)
$\text{HOCl} + h\nu \rightarrow \text{Cl} + \text{OH}$	(9)
$\text{ClO} + \text{NO}_2 + \text{M} \rightarrow \text{ClONO}_2 + \text{M}$	(10)
$\text{ClO} + \text{HO}_2 \rightarrow \text{HOCl} + \text{O}_2$	(11)
$\text{Cl} + \text{CH}_4 \rightarrow \text{HCl} + \text{CH}_3$	(12)
$\text{Cl} + \text{HO}_2 \rightarrow \text{HCl} + \text{O}_2$	(13)
<b>c</b>	
$\text{HCl} + \text{ClONO}_2 \rightarrow \text{Cl}_2 + \text{HNO}_3$	(14)

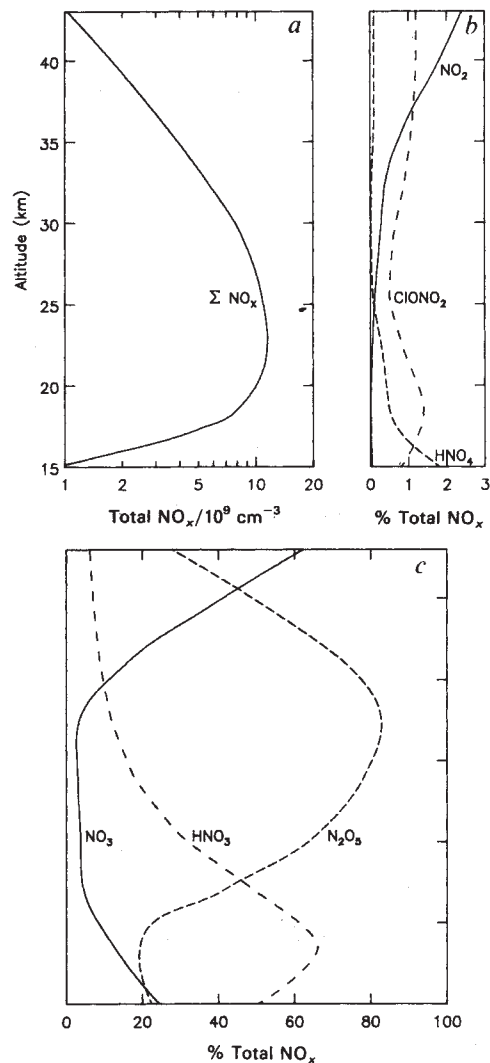


**Fig. 3**  $\text{NO}_x$  during the polar night. *a*, Total  $\text{NO}_x$   $\text{cm}^{-3}$ , from 15 to 43 km. *b*,  $\text{NO}_2$ ,  $\text{ClONO}_2$  and  $\text{HNO}_4$  as percentages of total  $\text{NO}_x$ . *c*,  $\text{NO}_3$ ,  $\text{HNO}_3$  and  $\text{N}_2\text{O}_5$  as percentages of total  $\text{NO}_x$ .

has large positive activation energy<sup>9</sup>, with the result that  $\psi$  is strongly dependent on  $[\text{ClO}]$  at low temperature, as shown in Fig. 4.  $[\text{ClO}]$  is not simply proportional to total  $\text{ClX}$ , because  $\text{ClONO}_2$  formation (reaction (10)) intervenes. Throughout the stratosphere,  $\chi \ll 1$ , so that  $[\text{ClO}] \sim [\text{Cl} + \text{ClO}]$ . From a steady-state analysis of the reactions given in Table 1b,

$$[\text{Cl} + \text{ClO}] \sim \frac{k_7[\text{HCl}][\text{OH}] + j_8[\text{ClONO}_2] + j_9[\text{HOCl}]}{k_{10}[\text{NO}_2] + k_{11}[\text{HO}_2] + \chi(k_{12}[\text{CH}_4] + k_{13}[\text{HO}_2])} \quad (4)$$

Values of  $\psi$ ,  $\chi$  and  $[\text{Cl} + \text{ClO}]$  obtained from equations (2), (3) and (4) are in good accord with full one-dimensional model results for late summer in Antarctica<sup>6</sup>. Neglecting seasonal effects other than those resulting from temperature and from variation of  $[\text{NO} + \text{NO}_2]$ , it is possible to solve simultaneously for  $[\text{NO}_2]$  and  $[\text{ClO}]$ , and to derive  $L$ . Results are shown in Table 2 as relaxation times<sup>8</sup>,  $[\text{O}_3]/L$ , for various conditions. The spring values (lines 2, 3 and 4) are highly dependent on  $\text{ClX}$  amount (compare columns *a* and *b*), the autumn values (line 1) much less so. At Argentine Islands, the sensitivity to  $\text{ClX}$  growth should resemble that seen in line 2, attributable solely to low temperature. Lines 3 and 4 show the enhanced sensitivity possible at stations within the Antarctic Circle, such as Halley Bay, arising from slow release of  $[\text{NO} + \text{NO}_2]$  following the polar night. It remains to be shown how stable  $\text{O}_3$  budgets were achieved with the relaxation times for the lower chlorine level (Table 2, *a*).

Much  $\text{O}_3$  destruction is driven by visible light, but production requires radiation below 242 nm. On the dates shown (Table 2), destruction persists for some 11 h, while, because of the long UV paths, production is weak (except around noon) at 29 km, and is virtually absent below that altitude. Line 1 of Table 2 then demands  $\text{O}_3$  transport in autumn from the upper to the lower stratosphere, which is consistent with inferred thermally-driven lagrangian-mean circulations<sup>10</sup>. A mean vertical velocity of 45 m per day is in good accord with calculations of net diabatic cooling<sup>11</sup> and gives a realistic total  $\text{O}_3$  decay rate in an otherwise conventional one-dimensional model<sup>6</sup>. The short

relaxation times in the lower stratosphere in autumn are tolerable, with adequate transport compensating for lack of  $\text{O}_3$  production.

In early spring, on the other hand, wave activity scarcely penetrates the cold dense core of the Antarctic polar vortex and with very low temperatures the net diabatic cooling is very weak<sup>11</sup>. Lagrangian transport in the vortex should then be almost negligible. (The virtual exclusion of Agung dust from the vortex supports this view<sup>5</sup>.) The final warming signals the end of this period of inactivity and is accompanied by large dynamically induced changes in  $\text{O}_3$  distribution. However, before the warming, with low chlorine, total  $\text{O}_3$  was in a state of near-neutral equilibrium, sustained primarily by the long relaxation times.

**Table 2** Relaxation times in days,  $[\text{O}_3]/L$ , for maximum chlorine levels 1.5 p.p.b.v. (*a*) and 2.7 p.p.b.v. (*b*) (1980)

Date	Altitude (km)	22		25.5		29		32.5		36		39.5		43	
		<i>a</i>	<i>b</i>	<i>a</i>	<i>b</i>	<i>a</i>	<i>b</i>	<i>a</i>	<i>b</i>	<i>a</i>	<i>b</i>	<i>a</i>	<i>b</i>	<i>a</i>	<i>b</i>
25 March	1	105	103	38	37	16	15	6.9	5.7	2.6	2.0	1.2	0.9	0.83	0.57
17 September	1	224	210	86	77	32	27	12.2	9.2	4.9	3.4	2.6	1.7	1.90	1.22
17 September	0.75	288	265	107	93	39	31	14.2	10.4	5.7	3.9	3.0	1.9	2.13	1.33
17 September	0.5	398	353	141	118	47	36	17.0	12.0	6.9	4.5	3.5	2.2	2.41	1.46

Noon values at 75.5°S, solar elevation 12.5°. Lower stratosphere at 230 K on 25 March; 190 K on 17 September. The altitudes shown apply to the summer temperature profile used in the model<sup>6</sup>.

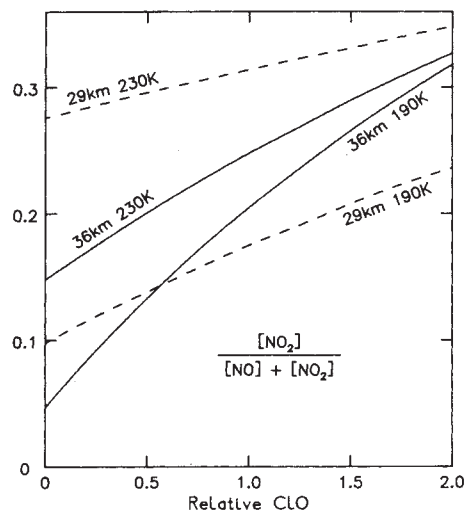


**Fig. 4**  $[\text{NO}_2]/[\text{NO} + \text{NO}_2]$  has the status of an efficiency factor for  $\text{O}_3$  destruction by the  $\text{NO}_x$  cycle. In terms of the ratio  $\psi$  in the text, it is  $\psi/(1 + \psi)$ . The figure shows how this factor varies with  $[\text{ClO}]$  at 190 K and at 230 K, at altitudes of 29 and 36 km. Values of  $[\text{O}_3]$ ,  $[\text{O}]$ ,  $[\text{ClO}]$  and  $j_3$  were taken from one-dimensional model results<sup>6</sup> (maximum chlorine 2.7 p.p.b.v.) for noon, 25 March at 75.5° S, solar elevation 12.5°. The abscissa is  $[\text{ClO}]$  relative to the model value. The rate-limiting reaction, (2) in Table 1, for the  $\text{NO}_x$  cycle has zero activation energy. Note how, nevertheless,  $\text{O}_3$  was protected against destruction by  $\text{NO}_x$  at low temperatures in a stratosphere with small amounts of ClX, but is losing this protection as ClX grows.

With higher chlorine, relaxation times of the order seen in line 4, Table 2, entail more rapid  $\text{O}_3$  losses. With negligible production below 29 km and only weak transport, large total  $\text{O}_3$  perturbation is possible. The extreme effects could be highly localized, restricted to the period with diurnal photolysis between polar night and the earlier of either the onset of polar day or the final spring warming. At the pole  $[\text{NO} + \text{NO}_2]$  rises continuously after the polar night, with the Sun. The final warming always begins over east Antarctica and spreads westwards across the pole. At Halley Bay the warming is typically some 14 days later than at the pole. Maximum  $\text{O}_3$  depletion could be confined to the Atlantic half of the zone bordered roughly by latitudes 70 and 80° S.

Comparable effects should not be expected in the Northern Hemisphere, where the winter polar stratospheric vortex is less cold and less stable than its southern counterpart. The vortex is broken down, usually well before the end of the polar night, by major warmings. These are accompanied by large-scale subsidence and strong mixing, in the course of which peak  $\text{O}_3$  values for the year are attained. Hence, sensitivity to ClX growth should be minimal if, as suggested above, this primarily results from  $\text{O}_3$  destruction at low temperatures in regions where  $\text{O}_3$  transport is weak.

We have shown how additional chlorine might enhance  $\text{O}_3$  destruction in the cold spring Antarctic stratosphere. At this time of the year, the long slant paths for sunlight make reservoir species absorbing strongly only below 280 nm, such as  $\text{N}_2\text{O}_5$ ,  $\text{ClONO}_2$  and  $\text{HO}_2\text{NO}_2$ , relatively long-lived. The role of these reservoir species should be more readily demonstrated in Antarctica, particularly the way in which they hold the balance between the  $\text{NO}_x$  and  $\text{ClO}_x$  cycles. An intriguing feature could be the homogeneous reaction (Table 1c) between HCl and  $\text{ClONO}_2$ . If this process has a rate constant as large as  $10^{-16} \text{ cm}^3 \text{ s}^{-1}$  (ref. 2) and a negligible temperature coefficient, the reaction would go almost to completion in the polar night, leaving inorganic chlorine partitioned between HCl and  $\text{Cl}_2$ , almost equally at 22 km for example. Photolysis of  $\text{Cl}_2$  at near-visible wavelengths would provide a rapid source of  $[\text{Cl} + \text{ClO}]$

at sunrise, not treated in equation (4). The polar-night boundary is, therefore, the natural testing ground for the theory of nonlinear response to chlorine<sup>1,2</sup>. It might be asked whether a nonlinear response is already evident (Fig. 2a). An intensive programme of trace-species measurements on the polar-night boundary could add greatly to our understanding of stratospheric chemistry, and thereby improve considerably the prediction of effects on the ozone layer of future halocarbon releases.

We thank B. A. Thrush and R. J. Murgatroyd for helpful suggestions.

Received 24 December 1984; accepted 28 March 1985.

1. Cicerone, R. J., Walters, S. & Liu, S. C. *J. geophys. Res.* **88**, 3647-3661 (1983).
2. Prather, M. J., McElroy, M. B. & Wofsy, S. C. *Nature* **312**, 227-231 (1984).
3. *The Stratosphere 1981, Theory and Measurements* (WMO Global Ozone Research and Monitoring Project Rep. No. 11, 1981).
4. Farman, J. C. & Hamilton, R. A. *Br. Antarct. Surv. Sci. Rep.* No. 90 (1975).
5. Farman, J. C. *Phil. Trans. R. Soc.* **B279**, 261-271 (1977).
6. Farman, J. C., Murgatroyd, R. J., Silnickas, A. M. & Thrush, B. A. *Q. Jl R. met. Soc.* (submitted).
7. McKenzie, R. L. & Johnston, P. V. *Geophys. Res. Lett.* **11**, 73-75 (1984).
8. Johnston, H. S. & Podolske, J. *Rev. Geophys. Space Phys.* **16**, 491-519 (1978).
9. *Chemical Kinetics and Photochemical Data for Use in Stratospheric Modelling, Evaluation No. 6* (JPL Publ. 83-62, 1983).
10. Dunkerton, T. *J. Atmos. Sci.* **35**, 2325-2333 (1978).
11. Dopplack, T. G. *J. Atmos. Sci.* **29**, 1278-1294 (1972).

## An Ordovician ophiolite in County Tyrone, Ireland

D. H. W. Hutton\*, M. Aftalion† & A. N. Halliday†

\* Department of Geological Sciences, University of Durham, Durham DH1 3LE, UK

† Scottish Universities Research and Reactor Centre, East Kilbride, Glasgow G75 0QU, UK

Ophiolites are regarded widely by geologists as remnants of old oceanic crust that has been obducted onto the continental margins during ocean or marginal basin closure and orogeny. Therefore, they provide evidence for the existence of old oceans and oceanic basins and are a key to the extension of plate tectonic modelling into pre-Mesozoic rock assemblages. In the Caledonide-Appalachian orogen, ophiolites are known although very few of these are dated well enough to provide accurate constraints on plate-tectonic kinematics. We report here the discovery of an ophiolitic sequence within the rocks of the Tyrone Igneous Complex in Northern Ireland. U/Pb dating combined with field evidence indicates that the Tyrone ophiolite was formed and then obducted onto the northern margins of the Iapetus Ocean close to 470 Myr BP (Arenig).

The Tyrone Igneous Complex (Fig. 1) occurs in an approximate along-strike continuation of the Midland Valley of Scotland; it is partly overlain by Upper Palaeozoic sediments within a shallow graben structure bounded by Dalradian rocks to the north and the Lower Palaeozoic of the Southern Uplands-Longford-Down zone to the south. The complex consists of three units (Fig. 1): a middle Ordovician (Llandeilo-Caradoc) volcanic sequence; a high metamorphic grade gneiss unit 'the central inlier'; and a unit of gabbros and dolerites previously called 'the basic plutonic complex'<sup>1</sup>. Opinions on the age relationships and significance of the units have varied. Originally the basic plutonic complex and volcanics were grouped together as Llandeilo-Caradoc and regarded as being altogether younger and in tectonic contact with the central gneisses<sup>2</sup>. Alternatively, the basic complex has been correlated with layered basic intrusions of Connemara and Aberdeenshire. This led to the view that both basic rocks and gneisses were older than and in unconformable contact beneath the Ordovician volcanic sequence<sup>3</sup>.